Two pion electroproduction with CLAS and baryon resonance analysis

M. Ripani,[1] V.D. Burkert,[2] V. Mokeev,[3] M. Battaglieri,[1] R. De Vita,[1] E. Golovach,[3] M. Taiuti,[1] G. Adams,[30] E. Anciant,[5] M. Anghinolfi,[1] D.S. Armstrong,[37] B. Asavapibhop,[23] G. Audit,[5] T. Auger,[5] H. Avakian,[2,17] H. Bagdasaryan,[38] J.P. Ball,[4] S. Barrow,[14] K. Beard,[20] M. Bektasoglu,[27] B.L. Berman,[15] N. Bianchi,[17] A.S. Biselli,[30] S. Boiarinov,[2,19] B.E. Bonner,[31] S. Bouchigny,[18,2] D. Branford,[12] W.J. Briscoe,[15] W.K. Brooks,[2] J.R. Calarco,[24] D.S. Carman,[26,7] B. Carnahan,[8] A. Cazes,[33] C. Cetina,[15] L. Ciciani,[27] R. Clark,[7] P.L. Cole,[34,2] A. Coleman,[37] D. Cords,[2] P. Corvisiero,[1] D. Crabb,[36] H. Crannell,[8] J.P. Cummings,[30] E. De Sanctis,[17] P.V. Degtyarenko,[2] H. Denizli,[28] L. Dennis,[14] K.V. Dharmawardane,[27] K.S. Dhuga,[15] C. Djalali,[33] G.E. Dodge,[27] D. Doughty,[9,2] P. Dragovitsch,[14] M. Dugger,[4] S. Dytman,[28] M. Eckhause,[37] H. Egiyan,[37] K.S. Egiyan,[38] L. Elouadrhiri,[2] A. Empl,[30] R. Fatemi,[36] G. Fedotov,[3] G. Feldman,[15] R.J. Feuerbach,[7] J. Ficenec,[35] T.A. Forest,[27] H. Funsten,[37] S.J. Gaff,[11] M. Gai,[10] M. Garçon,[5] G. Gavalian,[24,38] S. Gilad,[22] G.P. Gilfoyle,[32] K.L. Giovanetti,[20] P. Girard,[33] K. Griffioen,[37] M. Guidal,[18] M. Guillo,[33] V. Gyurjyan,[2] C. Hadjidakis,[18] J. Hardie,[9,2] D. Heddle,[9,2] P. Heimberg,[15] F.W. Hersman,[24] K. Hicks,[26] R.S. Hicks,[23] M. Holtrop,[24] J. Hu,[30] C.E. Hyde-Wright,[27] B. Ishkhanov,[3] M.M. Ito,[2] D. Jenkins,[35] K. Joo,[2,36] J.H. Kelley,[11] J.D. Kellie,[16] M. Khandaker,[25] D.H. Kim,[21] K.Y. Kim,[28] K. Kim,[21] M.S. Kim,[21] W. Kim,[21] A. Klein,[27] F.J. Klein,[8,2] M. Klusman,[30] M. Kossov,[19] L.H. Kramer,[13,2] Y. Kuang,[37] S.E. Kuhn,[27] J. Kuhn,[30] J. Lachniet,[7] J.M. Laget,[5] D. Lawrence,[23] Ji Li,[30] K. Livingston,[16] A. Longhi,[8] K. Lukashin,[2] J.J. Manak,[2] C. Marchand,[5] L.C. Maximon,[15] S. McAleer,[14] J. McCarthy,[36] J.W.C. McNabb,[7] B.A. Mecking,[2] M.D. Mestayer,[2] C.A. Meyer,[7] K. Mikhailov,[19] R. Minehart,[36] M. Mirazita,[17] R. Miskimen,[23] L. Morand,[5] S.A. Morrow,[18] V. Muccifora,[17] J. Mueller,[28] L.Y. Murphy,[15] G.S. Mutchler,[31] J. Napolitano,[30] R. Nasseripour,[13] S.O. Nelson,[11] S. Niccolai,[15] G. Niculescu,[26] I. Niculescu,[15] B.B. Niczyporuk,[2] R.A. Niyazov,[27] M. Nozar,[2,25] G.V. O'Rielly,[15] A.K. Opper,[26] M. Osipenko,[3] K. Park,[21] K. Paschke,[7] E. Pasyuk,[4] G. Peterson,[23] S.A. Philips,[15] N. Pivnyuk,[19] D. Pocanic,[36] O. Pogorelko,[19] E. Polli,[17] S. Pozdniakov,[19] B.M. Preedom,[33] J.W. Price,[6] Y. Prok,[36] D. Protopopescu,[24] L.M. Qin,[27] B.A. Raue,[13,2] G. Riccardi,[14] G. Ricco,[1] B.G. Ritchie,[4] F. Ronchetti,[17,29] P. Rossi,[17] D. Rowntree,[22] P.D. Rubin,[32] F. Sabatié,[5,27] K. Sabourov,[11] C. Salgado,[25] J.P. Santoro,[35,2] V. Sapunenko,[1] M. Sargsyan,[13,2] R.A. Schumacher,[7] V.S. Serov,[19] A. Shafi,[15] Y.G. Sharabian,[2,38] J. Shaw,[23] S. Simionatto,[15] A.V. Skabelin,[22] E.S. Smith,[2] L.C. Smith,[36] D.I. Sober,[8] M. Spraker,[11] A. Stavinsky,[19] S. Stepanyan,[27,38] P. Stoler,[30] I.I. Strakovsky,[15] S. Taylor,[31] D.J. Tedeschi,[33] R. Thompson,[28] L. Todor,[7] M. Ungaro,[30] M.F. Vineyard,[32] A.V. Vlassov,[19] K. Wang,[36] L.B. Weinstein,[27] A. Weisberg,[26] H. Weller,[11] D.P. Weygand,[2] C.S. Whisnant,[33] E. Wolin,[2] M.H. Wood,[33] L. Yanik,[15] A. Yegneswaran,[2] J. Yun,[27] B. Zhang,[22] J. Zhao,[22] Z. Zhou,[22]

[1] *INFN, Sezione di Genova, 16146 Genova, Italy*
[2] *Thomas Jefferson National Accelerator Laboratory, Newport News, Virginia 23606*
[3] *Moscow State University, 119899 Moscow, Russia*
[4] *Arizona State University, Tempe, Arizona 85287*
[5] *CEA-Saclay, Service de Physique Nucléaire, F91191 Gif-sur-Yvette, Cedex, France*
[6] *University of California at Los Angeles, Los Angeles, California 90095*
[7] *Carnegie Mellon University, Pittsburgh, Pennsylvania 15213*
[8] *Catholic University of America, Washington, D.C. 20064*
[9] *Christopher Newport University, Newport News, Virginia 23606*
[10] *University of Connecticut, Storrs, Connecticut 06269*
[11] *Duke University, Durham, North Carolina 27708*
[12] *Edinburgh University, Edinburgh EH9 3JZ, United Kingdom*
[13] *Florida International University, Miami, Florida 33199*
[14] *Florida State University, Tallahasee, Florida 32306*
[15] *The George Washington University, Washington, DC 20052*
[16] *University of Glasgow, Glasgow G12 8QQ, United Kingdom*
[17] *INFN, Laboratori Nazionali di Frascati, PO 13, 00044 Frascati, Italy*
[18] *Institut de Physique Nucleaire ORSAY, IN2P3 BP 1, 91406 Orsay, France*
[19] *Institute of Theoretical and Experimental Physics, Moscow, 117259, Russia*
[20] *James Madison University, Harrisonburg, Virginia 22807*
[21] *Kungpook National University, Taegu 702-701, South Korea*
[22] *Massachusetts Institute of Technology, Cambridge, Massachusetts 02139*
[23] *University of Massachusetts, Amherst, Massachusetts 01003*
[24] *University of New Hampshire, Durham, New Hampshire 03824*
[25] *Norfolk State University, Norfolk, Virginia 23504*
[26] *Ohio University, Athens, Ohio 45701*

[27] Old Dominion University, Norfolk, Virginia 23529
[28] University of Pittsburgh, Pittsburgh, Pennsylvania 15260
[29] Universita' di ROMA III, 00146 Roma, Italy
[30] Rensselaer Polytechnic Institute, Troy, New York 12180
[31] Rice University, Houston, Texas 77005
[32] University of Richmond, Richmond, Virginia 23173
[33] University of South Carolina, Columbia, South Carolina 29208
[34] University of Texas at El Paso, El Paso, Texas 79968
[35] Virginia Polytechnic Institute and State University, Blacksburg, Virginia 24061
[36] University of Virginia, Charlottesville, Virginia 22901
[37] College of William and Mary, Williamsburg, Virginia 23187 and
[38] Yerevan Physics Institute, 375036 Yerevan, Armenia

(Dated: July 30, 2002)

The cross section for the reaction $ep \to e'p\pi^+\pi^-$ was measured in the resonance region for 1.4<W<2.1 GeV and 0.5< Q^2 <1.5 GeV^2/c^2, using the CLAS detector at Jefferson Laboratory. Data shows resonant structures not visible in previous experiments. The comparison of our data to a phenomenological prediction using available information on N^* and Δ states shows an evident discrepancy. A better description of the data is obtained either by a sizeable change of the properties of the $P_{13}(1720)$ resonance or by introducing a new baryon state, not reported in published analyses.

PACS numbers: 13.60.Le, 13.40.Gp, 14.20.Gk

Electromagnetic excitation of nucleon resonances is sensitive to the spin and spacial structure of the transition, which in turn is connected to fundamental properties of baryon structure, like spin-flavour symmetries, confinement and effective degrees of freedom. In the mass region above 1.6 GeV many overlapping baryon states are present and some of them are not well known; measurement of the transition form factors of these states is important for our understanding of baryons. Many of these high-mass excited states tend to decouple from the single-meson channels and to decay predominantly in multipion channels, such as $\Delta\pi$ or $N\rho$, leading to $N\pi\pi$ final states [1]. Moreover, quark models with approximate (or "broken") SU(6)⊗O(3) symmetry [2, 3] predict more states than have been found experimentally; QCD mixing effects could decouple these unobserved states from the pion-nucleon channel [2], while strongly coupling them to two-pion channels [2, 4, 5]. These states would therefore not be observable in reactions with πN in the initial or final state. Other models such as the Quark Cluster Model [6] predict a fewer number of states than the symmetric model. Search for at least some of the "missing" states predicted in the most accepted quark models, and not predicted when using alternative symmetries, is crucial in discriminating between different models of baryon structure. Electromagnetic amplitudes for some missing states are predicted to be sizeable [2] as well. Therefore, exclusive double pion electroproduction is a fundamental tool in measuring poorly known states and possibly observing new ones.

In this paper we report a measurement of the $ep \to e'p\pi^+\pi^-$ reaction studied with the CEBAF Large Acceptance Spectrometer (CLAS) at Jefferson Lab. Typical beam currents of a few nA were delivered to Hall B on a liquid hydrogen target, corresponding to luminosities up to $4 \cdot 10^{33}$ cm^{-2}s^{-1}. Data were taken in 1999 for about two months at beam energies of 2.6 and 4.2 GeV. Important features of the CLAS [7] are its large kinematic coverage for multi-charged-particle final states and its good momentum resolution ($\Delta p/p \sim 1\%$); using an inclusive electron trigger based on a coincidence between the forward electromagnetic shower calorimeter and the gas Cerenkov detector, many exclusive hadronic final states were measured simultaneously. Scattered electrons were identified through cuts on the calorimeter energy loss and the Cerenkov photo-electron distribution. Different channels were separated through particle identification using time-of-flight information and other kinematic cuts. We used the missing-mass technique, requiring detection in CLAS of at least $ep\pi^+$. The good resolution obtained allowed selection of the exclusive final state $ep\pi^+\pi^-$ After applying fiducial cuts to define the detector volume, the data sample was reduced to about $2 \cdot 10^5$ two pion events. The range of invariant hadronic center-of-mass (CM) energy W (in 25 MeV bins) was 1.4-1.9 GeV for two bins in the invariant momentum transfer Q^2 from 0.5-0.8 (GeV/c)^2 and 0.8-1.1 (GeV/c)^2, and 1.4-2.1 GeV for the highest Q^2 bin, 1.1-1.5 (GeV/c)^2. Data were corrected for acceptance, reconstruction efficiency, radiative effects, and empty target counts. They were further binned in the following set of hadronic CM variables: invariant mass of the $p\pi^+$ pair (10 bins), invariant mass of the $\pi^+\pi^-$ pair (10 bins), π^- polar angle θ (10 bins), azimuthal angle ϕ (5 bins), and rotation freedom ψ of the $p\pi^+$ pair with respect to the hadronic plane (5 bins). The full differential cross section is therefore of the form:

$$\frac{d\sigma}{dW dQ^2 dM_{p\pi^+} dM_{\pi^+\pi^-} dcos\theta_{\pi^-} d\phi_{\pi^-} d\psi_{p\pi^+}} =$$
$$\Gamma_v \frac{d\sigma_v}{dM_{p\pi^+} dM_{\pi^+\pi^-} dcos\theta_{\pi^-} d\phi_{\pi^-} d\psi_{p\pi^+}} = \Gamma_v \frac{d\sigma_v}{d\tau} \qquad (1)$$

$$\Gamma_v = \frac{\alpha}{4\pi} \frac{1}{E^2 M_p^2} \frac{W(W^2 - M_p^2)}{(1-\epsilon) Q^2} \qquad (2)$$

where Γ_v is the virtual photon flux, $\frac{d\sigma_v}{d\tau}$ is the virtual photon cross section, α is the fine structure constant, E is the electron beam energy, M_p is the proton mass, and ϵ is the virtual photon transverse polarisation [8]. Systematic uncertainties were estimated as a function of W and Q^2. The main sources were acceptance modeling, numerical integration, and radiative corrections modeling, being at the 3 to 10% level. The various cuts applied (fiducial, missing mass, etc.) contributed 2 to 5%. In Fig. 1 (left) we report the total virtual photon cross section as a function of W for all Q^2 intervals analyzed. The CLAS data points clearly exhibit structures, not visible in previous data [9] due to limited statistical accuracy.

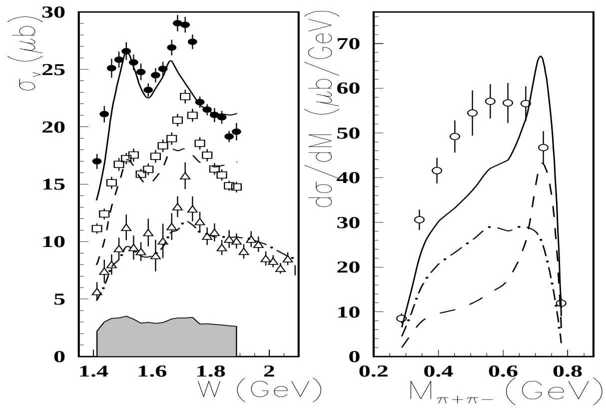

FIG. 1: Left: total cross section for $\gamma_v p \rightarrow p\pi^+\pi^-$ as a function of W. Data from CLAS are shown at Q^2=0.5-0.8 (GeV/c)^2 (full points), Q^2=0.8-1.1 (GeV/c)^2 (open squares), and Q^2=1.1-1.5 (GeV/c)^2 (open triangles). Error bars are statistical only, while the bottom band shows the sytematic error for the lowest Q^2 bin. The curves represent our step (A) reference calculations. Right: $\frac{d\sigma_v}{dM_{\pi^+\pi^-}}$ from CLAS at Q^2=0.8-1.1 (GeV/c)^2 and W=1.7-1.725 GeV (statistical error bars only). The curves represent our step (A) reference calculations, extrapolated to the edge points. The dashed line includes all resonances, the dot-dashed line includes only the non-resonant part, and the solid line is the full calculation.

Since existing theoretical models[10] are limited to W <1.6 GeV, for a first interpretation of the data we employed a phenomenological calculation [11] describing the reaction $\gamma_v p \rightarrow p\pi^+\pi^-$ in the kinematic range of interest as a sum of amplitudes for $\gamma_v p \rightarrow \Delta\pi \rightarrow p\pi^+\pi^-$ and $\gamma_v p \rightarrow \rho^0 p \rightarrow p\pi^+\pi^-$, while possible other mechanisms were parameterized as phase space. A detailed treatment was developed for the non-resonant contributions to $\Delta\pi$, while for ρp production they were described through a simple diffractive ansatz. For the resonant part, a total of 12 states classified as 3* and 4* [1], with sizeable $\Delta\pi$ and/or ρp decays were included, based on a Breit-Wigner ansatz. A few model parameters, representing non-resonant production and the phase space part, were fitted to CLAS data and kept fixed in the subsequent analysis. To simplify the fits, we reduced eqn. (1) to single-differential cross sections, integrating over four hadronic variables. Then, 3 such differential cross sections with the largest binning were fitted simultaneously, $\frac{d\sigma_v}{dM_{p\pi^+}}$ (connected to $\pi^-\Delta^{++}$ production), $\frac{d\sigma_v}{dM_{\pi^+\pi^-}}$ (connected to $\rho^0 p$ production) and $\frac{d\sigma_v}{d\theta_{\pi^-}}$ (primarily connected to $\pi^-\Delta^{++}$ production that is dominant in this energy region). When fitting the data, we calculated a χ^2 per degree of freedom (χ^2/ν) for all Q^2 values and in the restricted W range where we focused our analysis, as discussed in the following paragraphs. For each W and Q^2 bin, 26 data points from the 3 mentioned differential cross sections were used (2 edge points in each of the mass distributions were excluded as the model did not take into account the kinematic smearing in the $M_{\pi^+\pi^-}$ vs $M_{p\pi^+}$ Dalitz plot, caused by the W bin width). Schematically, the data analysis was performed in the following steps: (A) We produced reference curves using available information on resonances. Discrepancies between the CLAS data and our calculation were observed which led to the subsequent steps B and C. (B) Data around W=1.7 GeV were fitted in different ways. The best fit, corresponding to a prominent P_{13} partial wave, could be attributed to the PDG $P_{13}(1720)$ resonance, but with significantly modified parameters with respect to the literature. (C) As an alternative description, we introduced a new baryon state around 1.7 GeV. In what follows we describe each of the steps above in more detail.

Step (A) - To produce reference curves, the electromagnetic couplings $A_{1/2}$,$A_{3/2}$ were taken from a parameterization of the Q^2 evolution for several states extracted from previous experiments, and from Single Quark Transition Model (SQTM) fits [12] for states where no data were available. For the $P_{11}(1440)$ (Roper), given the scarce available data, the amplitude $A_{1/2}$ was taken from a Non-Relativistic Quark Model (NRQM) [13]. Partial LS decay widths were taken from a previous analysis of hadronic data [14] and renormalised to total widths from Ref. [1]. Results for step (A) are reported in Fig. 1 (left). The strength of the $D_{13}(1520)$ resonance at 1.5 GeV and the underlying continuum are well reproduced, except for the region on the low-mass side of the peak. However, a strong discrepancy is evident at W around 1.7 GeV. Moreover, at this energy the reference curve exhibits a strong peak in the pion-pion invariant mass (Fig. 1, right), connected to sizeable ρ meson production. This contribution was traced back to the 80-90% branching ratio of the $P_{13}(1720)$ into this channel [1, 14, 15].

Step (B) - Starting from the above mentioned reference values, the parameters of various states were varied in order to fit the CLAS data. In this discussion, we restrict ourselves to the discrepancy around 1.7 GeV and the few resonant states relevant in this energy region. All χ^2/ν values were calculated from the 8 W bins between 1.64 and 1.81 GeV and from the 3 Q^2 bins (624 data points). There were typically 23 free parameters cor-

TABLE I: PDG $P_{13}(1720)$ parameters from fit (B) and new state parameters from fit (C). Errors are statistical.

	M (MeV)	Γ (MeV)	$\frac{\Gamma_{\pi\Delta}}{\Gamma}$ (%)	$\frac{\Gamma_{\rho N}}{\Gamma}$ (%)
PDG P_{13} (B)	1725±20	114±19	63±12	19±9
PDG [1]	1650-1750	100-200	N/A	70-85
new P_{13} (C)	1720±20	88±17	41±13	17±10

responding to 601 d.o.f. Assuming the resonance properties given by the PDG, such a bump cannot be due to the $D_{15}(1675)$, $F_{15}(1680)$, or $D_{33}(1700)$; the first because its well known position cannot match the peak; the second because of precisely known position and photocouplings [16]; the third due to its large width ($\sim$ 300 MeV). The remaining possibilities from PDG were the $D_{13}(1700)$, the $P_{13}(1720)$ and the $P_{11}(1710)$, for which no data on $A_{1/2,3/2}$ at $Q^2 > 0$ are available [16]. If no configuration mixing occurs, the $D_{13}(1700)$ cannot be excited at all in an SQTM, while the SQTM prediction for the $P_{13}(1720)$ relies on ad hoc assumptions. According to the literature [1, 14, 15], hadronic couplings of the $D_{13}(1700)$ and total width of the $P_{11}(1710)$ are poorly known, while the $P_{13}(1720)$ hadronic parameters should be better established. Several other partial waves were investigated in step (C), under different assumptions.

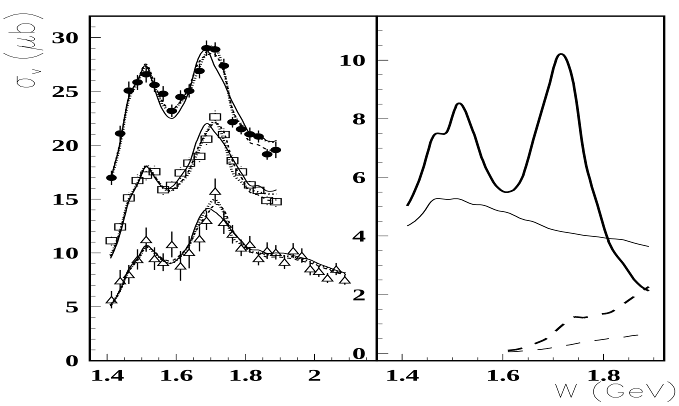

FIG. 2: Left: Total cross section for $\gamma_v p \rightarrow p\pi^+\pi^-$ as a function of W from CLAS at the 3 mentioned Q^2 intervals (see fig.1). The error bars are statistical only. The curves (see text) correspond to step (B) when fitting the bump with $D_{13}(1700)$ (solid), $P_{13}(1720)$ (dashed) or $P_{11}(1710)$ (dotted). Right: subdivision of the fitted cross section (B) for Q^2=0.5-0.8 (GeV/c)^2 into $\Delta^{++}\pi^-$ resonant (thick solid), $\Delta^{++}\pi^-$ continuum (thin full line), $\rho^0 p$ resonant (thick dashed), and $\rho^0 p$ continuum (thin dashed). Notice the different vertical scales.

To improve our reference curves before fitting the bump: the $P_{11}(1440)$ strength was fitted to the low W data; the $D_{15}(1675)$ and the $D_{13}(1700)$ photocouplings, vanishing in the SQTM, were replaced by NRQM values from [13]; an empirically established $A_{1/2,3/2}$ SQTM fitting uncertainty of 10-20 % (σ) was applied to all N^* states; a 20 % fluctuation was applied to the $A_{1/2,3/2}$ NRQM values of the $D_{13}(1700)$; the hadronic parameters were allowed to vary for the $D_{13}(1700)$, according to [14]; finally, the curves closest to the data were selected as starting point. We then performed three separate fits, in which either the $D_{13}(1700)$ or the $P_{13}(1720)$ or the $P_{11}(1710)$ parameters were varied. More precisely, hadronic parameters for $D_{13}(1700)$ were allowed to vary in all fits because of their large uncertainty from [14]. Our procedure was to apply iteratively: a wide variation of $A_{1/2,3/2}$ for the single resonance involved in the fit; a wide variation of its hadronic parameters; a variation of the $D_{13}(1700)$ hadronic parameters inside uncertainties. While all 3 states gave reasonable overall fits of the W spectrum and the Q^2 dependence (Fig. 2), the preferred solution was the $P_{13}(1720)$. In particular, in the other two fits, the description of angular distributions and/or of the $\pi\pi$ invariant mass was poor (Fig. 3), with a χ^2/ν of 5.2 for the $D_{13}(1700)$ and 4.3 for the $P_{11}(1710)$. Instead, in the $P_{13}(1720)$ fit, a better description of all 3 fitted distributions was obtained (Fig. 3), with χ^2/ν=3.4. However, the resulting values for the branching fractions were significantly different from previous analyses reported in the literature and well outside the reported errors [1, 14, 15]. Table I shows our results (first row) with statistical uncertainties, in comparison with the PDG values. In Table II (first 3 rows) we report the corresponding $A_{1/2,3/2}$ values for the $P_{13}(1720)$ fit. The error reflects statistical uncertainties in the data and correlations among different resonances. We then tested the reliability of the fits by varying the photocouplings of all states by 80 % (σ). The new best values of $A_{1/2,3/2}$ coincided with the previous ones within the errors.

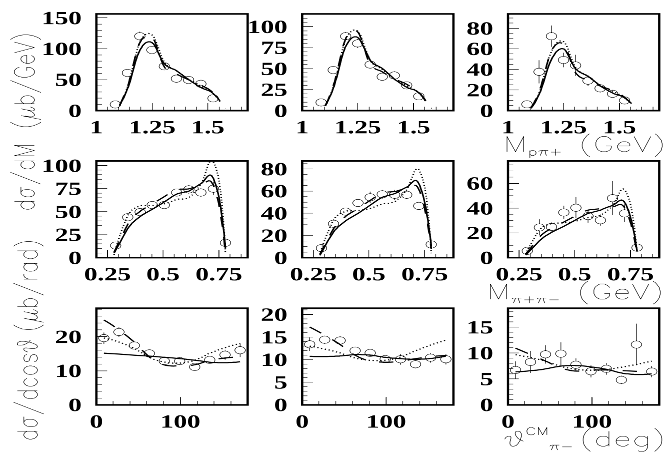

FIG. 3: $\frac{d\sigma_v}{dM_{p\pi^+}}$, $\frac{d\sigma_v}{dM_{\pi^+\pi^-}}$ and $\frac{d\sigma_v}{d\theta_{\pi^-}}$ from CLAS (from top to bottom) at W=1.7-1.725 GeV and for the 3 mentioned Q^2 intervals (left to right). The error bars include statistical errors only. Curves (see text) correspond to step (B) when fitting the 1.7 GeV bump with $D_{13}(1700)$ (solid), $P_{13}(1720)$ (dashed) or $P_{11}(1710)$ (dotted) and are extrapolated to the mass distributions edge points.

As discussed above, fitting data around 1.7 GeV with established baryon states either leads to a poor fit or to a drastic change in resonance parameters with respect to published analyses. On the other hand, in the framework

TABLE II: PDG $P_{13}(1720)$ photocouplings from fit (B) (first 3 rows) and new state photocouplings from fit (C) (last 3 rows). Errors are statistical.

Q^2 $(\mathrm{GeV/c})^2$	$A_{1/2}$ $(10^{-3}/\sqrt{GeV})$	$A_{3/2}$ $(10^{-3}/\sqrt{GeV})$
0.65	2±21	-83±5
0.95	3±29	-63±8
1.30	2±12	-45±27
0.65	15±25	-74±8
0.95	12±20	-53±6
1.30	3±14	-41±18

of our analysis, we have no possibility to assess the reliability of the previously determined hadronic parameters of the PDG $P_{13}(1720)$. We have to remark at this point that the source of the hadronic parameters is the reaction $\pi N \to \pi\pi N$, while the CLAS data are based on an electromagnetic probe in the initial channel. Therefore the resonant content seen in the two reactions may be different. In particular, the conventional $P_{13}(1720)$ state may be not well visible in two pion electroproduction, while some other state may manifest in such reaction as a result of the different entrance channel. Therefore we further investigated this possibility, checking whether our data could be fitted by including another baryon state, not reported before, but still accomodating the known baryons with their published hadronic properties. Therefore, in step (C) we introduced a new baryon state, while keeping hadronic parameters of the $P_{13}(1720)$ as in Refs. [1, 14]. Quantum numbers S_{I1},P_{I1},P_{I3},D_{I3},D_{I5}, F_{I5},F_{I7} were tested on an equal footing, I being the isospin, undetermined in our measurement. We then varied simultaneously photocouplings of the new state and hadronic parameters of new state and $D_{13}(1700)$. The new state total decay width was varied in the range 40-600 MeV, while the position range was 1.68-1.76 GeV. The best fit was obtained with a P_{I3} state, with a χ^2/ν=3.3, while other solutions gave a $\chi^2/\nu \geq 4.2$. A good fit quality was obtained, while keeping the $P_{13}(1720)$ hadronic parameters at published values. Curves obtained from the best fit were nearly identical with the dashed lines in Figs. 2 and 3. In order to avoid the unobserved ρ production peak (Fig. 1, right), the photocouplings of the PDG $P_{13}(1720)$ had to be reduced by about a factor of two with respect to the SQTM prediction, making its contribution very small. Instead, in this fit the main contribution to the bump was coming from the new state. Resonance parameters and $A_{1/2,3/2}$ values obtained for the new state hypothesis are reported in Table I (last row) and II (last 3 rows), respectively. A second P_{13} state is indeed predicted in the quark model by Capstick and Roberts [4], however with a mass of 1870 GeV. The presence of a new 3-quark state with the same quantum numbers as the conventional $P_{13}(1720)$ in the same mass range would likely lead to strong mixing. However, as mentioned above, a different isospin and/or partial wave cannot be excluded. Finally, the new state may have a different internal structure, such as a hybrid baryon with excited glue components. Such a P_{13} hybrid state is predicted in the flux tube model [17]. Yet another possibility is that some resonance parameters established in previous analyses may have much larger uncertainties than reported in the literature, under closer inspection. In this case, outlined in our step (B), our analysis would establish new, more precise parameters for a known state, and invalidate previous results.

In conclusion, we analysed CLAS data on $ep \to e'p\pi^+\pi^-$ within a particular phenomenological model. In a direct comparison with our prediction using available resonance information, the observed bump at 1.7 GeV was not reproduced. In a first fit based only on established resonances from PDG, we found that the $P_{13}(1720)$ resonance was reproducing the observed peak and angular distributions reasonably well, when significantly changing its decay pattern with respect to the published analyses. The extracted photocouplings were quite different from the SQTM prediction. In an alternative fit, we used the published $P_{13}(1720)$ strong parameters, while reducing its photocouplings by about a factor of two with respect to the SQTM. In this case, the bump at 1.7 GeV was fitted by introducing a new resonance. In both cases, photocouplings of the $P_{13}(1720)$ PDG state at $Q^2 > 0$ were derived for the first time. Our best fit for the hypothetical new state corresponds to positive parity and spin $\frac{3}{2}$, while isospin could not be determined. It is relatively narrow and has a sizeable $\Delta\pi$ and a small ρN decay coupling, at variance with published properties of the established $P_{13}(1720)$. A simultaneous analysis of single and double pion processes provides more constraints and may help to better discriminate between alternative interpretations of the observed resonance structure in the CLAS data. Such an effort is currently under way.

We would like to acknowledge the outstanding efforts of the staff of the Accelerator and the Physics Divisions at JLab that made this experiment possible. This work was supported in part by the Istituto Nazionale di Fisica Nucleare, the French Commissariat à l'Energie Atomique, the U.S. Department of Energy and National Science Foundation, and the Korea Science and Engineering Foundation. The Southeastern Universities Research Association (SURA) operates the Thomas Jefferson National Accelerator Facility for the United States Department of Energy under contract DE-AC05-84ER40150.

[1] D.E. Groom *et al.*, Eur. Phys. J **C 15**, 1 (2000).
[2] R. Koniuk and N. Isgur, Phys. Rev. Lett. **44**, 845 (1980);

Phys. Rev. **D21**, 1868 (1980).
[3] M.M. Giannini, Rep. Prog. Phys. **54**, 453 (1990).
[4] S. Capstick and W. Roberts, Phys. Rev. **D49**, 4570 (1994).
[5] F. Stancu and P Stassart, Phys. Rev. **D47**, 2140 (1993).
[6] K.F. Liu and C.W. Wong, Phys. Rev. **D28**, 170 (1983).
[7] W. Brooks, Proc. of PANIC '99, Uppsala, Sweden, 10-16 June 1999, Nucl. Phys. **A 663&664**, 29c (2000).
[8] E. Amaldi, S. Fubini, and G. Furlan, Pion Electroproduction, Springer Tracts in Modern Physics **83** (1989).
[9] V. Eckart *et al.*, Nucl. Phys. **B55**, 45 (1973); P. Joos *et al.*, Phys. Lett. **B52**, 481 (1974); K. Wacker *et al.*, Nucl. Phys. **B144**, 269 (1978).
[10] J.C. Nacher and E. Oset, Nucl. Phys. **A674**, 205 (2000)
[11] V. Mokeev *et al.*, Phys. of Atomic Nucl. **64**, 1292 (2001).
[12] V.D. Burkert, Czech. Journ. of Phys. **46**, 627 (1996).
[13] F. Close and Z.P. Li, Phys. Rev. **D42**, 2194 (1990).
[14] D.M. Manley and E.M. Salesky, Phys. Rev. **D45**, 4002 (1992).
[15] T.P. Vrana *et al.*, Phys. Rept. **328**, 181 (2000).
[16] V. Burkert, Nucl. Phys. **A684**, 16 (2001).
[17] P. Page, in Proceedings of "NSTAR2000: Excited Nucleons and Hadronic Structure", Newport News, VA, 16-19 Feb. 2000, World Scientific, eds. V. Burkert, L. Elouadrhiri, J. Kelly, and R. Minehart.